

PACS numbers: 52.38.Ph; 52.25.Os; 52.59.Px; 52.50.Jm
DOI: 10.1070/QE2013v043n03ABEH015102

Simulation of the generation of the characteristic X-ray emission by hot electrons in a foil

O.F. Kostenko, N.E. Andreev

Abstract. **We have developed a model to calculate the yield of the characteristic X-ray radiation from a foil, taking into account the dependence of the average energy and the number of hot electrons on the intensity of the laser pulse, the self-absorption of X-rays and the effect of refluxing of hot electrons. The yield of K_α radiation from a silver foil is optimised at relativistic intensities. A method is proposed for diagnosing the effect of electron refluxing, which greatly increases the yield of K_α radiation.**

Keywords: *hot electrons, refluxing, generation and absorption of K_α radiation, foil.*

1. Introduction

Hot electrons produced by irradiating a solid target by a relativistically intense laser pulse [1] penetrate into the target and ionise the K-shell of atoms, which leads to the emission of characteristic X-rays on 2p–1s transitions in excited atoms. The generated short-pulse K_α radiation can be used, for example, to diagnose a dense plasma (see reviews [2, 3]). Of importance here is the problem of increasing the number of generated photons and their energy [2]. The K_α yield can be increased by increasing laser pulse energy and efficiency of its conversion to the energy of this radiation. At relativistic intensities, the efficiency, achieved through the use of isolated thin foils with limited transverse dimensions, in which hot electrons are trapped and refluxing, is much greater than in the case of foils placed on a massive conductor, which due to the return current of cold electrons compensates for the charge of fast electrons leaving the foil [3–5]. In these papers the results of measurements of the coefficient of the laser pulse energy conversion into the K_α radiation energy were compared with the results of model calculations, taking into account the loss of energy of the hot electrons in the foil, the cross section of the K-shell ionisation by an electron impact and the probability of K_α radiation de-excitation by excited atoms. The energy distribution of the electrons impinging onto the foil was determined by measuring the bremsstrahlung spectrum and by using calculations by the particle-in-cell (PIC) method [3] or was considered exponential with the temperature defined by the ponderomotive potential [3–5]. In the latter case it was assumed that the electron temperature T_h depends on the peak intensity, and the conversion efficiency of the laser energy into the energy of hot electrons η is constant over a wide range of intensities – from sub-relativistic to ultra-relativistic. K_α radiation absorption in thin foils was assessed using a constant factor.

In this paper, we construct a model that takes into account the K_α radiation absorption in the foils of arbitrary thickness with and without electron refluxing and the dependences of η and T_h on the laser pulse intensity. We have obtained the dependences of the anisotropic photon yield from the front and rear sides of the foil (per unit laser energy and per unit solid angle) on the foil thickness and the peak intensity. The calculations have been performed for a silver foil (the photon energy of K_α radiation is 22.1 keV) at intensities corresponding to the experiment conducted on the PHELIX laser facility [3].

2. Description of the model

An electron with energy E_0, incident on a foil of thickness d (perpendicular to its surface), generates

$$\mathrm{d}n_K = \omega_K p_\alpha n_a \sigma_K(E)\mathrm{d}x$$

K_α photons on a path $\mathrm{d}x$ at a distance x from its surface, where $\sigma_K(E)$ is the impact ionisation cross section of the K-shell by an electron with energy $E(E_0, x)$; n_a is the concentration of atoms; ω_K is the probability of radiative de-excitation; and p_α is the probability of the K_α fluorescence yield. In this case, from front side of the foil at an angle α_0 to the normal

$$\mathrm{d}n_{em} = \mathrm{d}n_K \frac{\mathrm{d}\Omega}{4\pi}\exp\Big(-\frac{x}{l_a\cos\alpha_0}\Big)$$

photons are emitted into a solid angle $\mathrm{d}\Omega$, where l_a is the absorption length. The electron energy loss is described by the function $S_p(E)$:

$$\frac{\mathrm{d}E}{\mathrm{d}x} = -S_p(E).$$

The electron mean free path in a solid, where its energy decreases from E_0 to the ionisation potential of the K-shell E_K, is

$$l_e(E_0) = \int_{E_K}^{E_0}\frac{\mathrm{d}E}{S_p(E)},$$

whence $x = l_e(E_0) - l_e(E)$.

If $l_e(E_0) \leqslant d$, then the total number of photons emitted by the electron per unit solid angle in the direction determined by the angle α_0 is

O.F. Kostenko, N.E. Andreev Joint Institute for High Temperatures, Russian Academy of Sciences, ul. Izhorskaya 13, Bld. 2, 125412 Moscow, Russia; e-mail: olegkost@ihed.ras.ru, andreev@ras.ru

Received 24 December 2012; revision received 12 February 2013
Kvantovaya Elektronika **43** (3) 237–241 (2013)
Translated by I.A. Ulitkin

$$\frac{dN^{f}_{em}(E_0)}{d\Omega} = \frac{\omega_K p_\alpha n_a}{4\pi}\int_{E_K}^{E_0}\frac{\sigma_K(E)}{S_p(E)}dE$$

$$\times\exp\left[-\frac{l_e(E_0)-l_e(E)}{l_a\cos\alpha_0}\right]. \quad (1)$$

Therefore, the number of the photons emitted from the back side of the foil per unit solid angle at an angle β_0 to the normal is equal to

$$\frac{dN^{b}_{em}(E_0)}{d\Omega} = \frac{\omega_K p_\alpha n_a}{4\pi}\int_{E_K}^{E_0}\frac{\sigma_K(E)}{S_p(E)}dE$$

$$\times\exp\left\{-\frac{d-[l_e(E_0)-l_e(E)]}{l_a\cos\beta_0}\right\}. \quad (2)$$

If the electron, after reaching the back side of the foil at $l_e(E_0) > d$, leaves it, then in Eqns (1) and (2) the lower limit of integration E_K is replaced by the energy E_f, which is found from the solution of the equation $l_e(E_0) - l_e(E_f) = d$. If the electron refluxes in the foil at $l_e(E_0) > d$, then

$$\frac{dN^{f}_{em}(E_0)}{d\Omega} = \frac{\omega_K p_\alpha n_a}{4\pi}\sum_{i=1}^{N+1}\int_{E_i}^{E_{i-1}}\frac{\sigma_K(E)}{S_p(E)}dE$$

$$\times\exp\left\{\frac{(2p_i-1)[l_e(E)-l_e(E_{i-1})]-(1-p_i)d}{l_a\cos\alpha_0}\right\}, \quad (3)$$

$$\frac{dN^{b}_{em}(E_0)}{d\Omega} = \frac{\omega_K p_\alpha n_a}{4\pi}\sum_{i=1}^{N+1}\int_{E_i}^{E_{i-1}}\frac{\sigma_K(E)}{S_p(E)}dE$$

$$\times\exp\left\{\frac{(1-2p_i)[l_e(E)-l_e(E_{i-1})]-p_i d}{l_a\cos\beta_0}\right\}, \quad (4)$$

where $N = [l_e(E_0)/d]$; $p_i = i - 2[i/2]$, i.e., p_i is equal to unity if i is an odd number, and to zero if i is an even number. When $i \in 1,\ldots,N$, the energy E_i is found by solving the equation $l_e(E_0) - l_e(E_i) = id$, and $E_{N+1} = E_K$.

The spectrum of the hot electrons incident on the foil was described by an exponential energy distribution

$$dn_e = \frac{dN_e}{T_h(I_L)}\exp\left[-\frac{E_0}{T_h(I_L)}\right] \quad (5)$$

with an average energy determined by the ponderomotive potential [1]

$$T_h(I_L) = mc^2\{[1+a_L(I_L)^2]^{1/2}-1\},$$

where $a_L(I_L) = 0.855\,(I_L/10^{18}\ \mathrm{W\,cm^{-2}})^{1/2}\,(\lambda/1\ \mu\mathrm{m})$ is the normalised amplitude of the laser field; $I_L(r,t)$ is the intensity of the laser pulse in the focal spot; and λ is the wavelength. The number of electrons dN_e was found from the law of conservation of energy

$$dN_e T_h(I_L) = \eta(I_L)dE_L, \quad (6)$$

where $\eta(I_L)$ is the conversion efficiency of the laser energy

$$dE_L = I_L(r,t)2\pi r dr dt \quad (7)$$

into the energy of hot electrons.

It follows from formulas (5)–(7) that the laser pulse generates

$$\frac{dN_K}{d\Omega} = 2\pi\int_0^\infty r dr\int_{-\infty}^{\infty}dt\frac{\eta(I_L)I_L(r,t)}{T_h^2(I_L)}\int_{E_K}^{\infty}dE_0$$

$$\times\exp\left[-\frac{E_0}{T_h(I_L)}\right]\frac{dN_{em}(E_0)}{d\Omega} \quad (8)$$

photons per unit solid angle, where $dN_{em}(E_0)/d\Omega$ is defined by expressions (1)–(4), as appropriate. In the case of the Gaussian intensity distribution

$$I_L(v) = I_0 e^{-v}, \quad v = \frac{r^2}{r_0^2}+\frac{t^2}{t_0^2}$$

formula (8) takes the form

$$\frac{dN_K}{d\Omega} = 2\pi r_0^2 t_0 I_0\int_0^\infty\sqrt{v}\,dv\frac{\eta(v)e^{-v}}{T_h^2(v)}$$

$$\times\int_{E_K}^{\infty}dE_0\exp\left[-\frac{E_0}{T_h(v)}\right]\frac{dN_{em}(E_0)}{d\Omega}.$$

It follows from (7), the laser pulse energy is $E_L = \pi^{3/2}r_0^2 t_0 I_0$; therefore,

$$N_{K\alpha} = \frac{1}{E_L}\frac{dN_K}{d\Omega} = \frac{2}{\sqrt{\pi}}\int_0^\infty\sqrt{v}\,dv\frac{\eta(v)e^{-v}}{T_h^2(v)}$$

$$\times\int_{E_K}^{\infty}dE_0\exp\left[-\frac{E_0}{T_h(v)}\right]\frac{dN_{em}(E_0)}{d\Omega} \quad (9)$$

photons per unit laser energy are emitted in a given direction per unit solid angle.

3. Simulation results

Calculations by formula (9) were performed at intensities $I_0 = 5\times10^{17}$–1.5×10^{19} W cm^{-2} ($\lambda = 1.053$ μm), which correspond to experiments carried out on the PHELIX laser facility with a pulse duration of ~700 fs [3]. In accordance with paper [6], in the case of normal incidence of a high intensity laser pulse ($I_L\lambda^2 \approx 10^{17}$ W cm^{-2} μm^2 and higher) the generation of hot electrons is due to the oscillatory component of the ponderomotive force directed along the gradient of concentration of thermal electrons. The comparison of the dependences of hot electron temperature on $I_L\lambda^2$ with the results of measurements performed upon interaction of the different femtosecond laser pulses with solid targets, shows [7] that at such intensities there occurs a transition to ponderomotive scaling [1]. Laser energy conversion coefficient $\eta(I_L)$ was determined by fitting the results of PIC calculations (Fig. 1), which were carried out for a 700-fs laser pulse incident at a small angle. The integration interval in the variable v is limited from above by $v_{max} = \ln(I_0/I_L^*)$, which corresponds to the condition $\eta(I_L) = 0$ at $I_L \leqslant I_L^* \approx 5\times10^{16}$ W cm^{-2}. The upper limit of integration over energy E_0 is chosen equal to $9T_h(v)$, taking into account the results of measurements and PIC simulations [3].

Energy loss of electrons in silver $S_p(E)$ was calculated using the ESTAR database [8]. The cross section of the K-shell ionisation, $\sigma_K(E)$, is determined according to the analytical expression [9], in which the corresponding factor [10, 11] takes into account the growth of the cross section with increasing energy of the relativistic electrons. In the calcula-

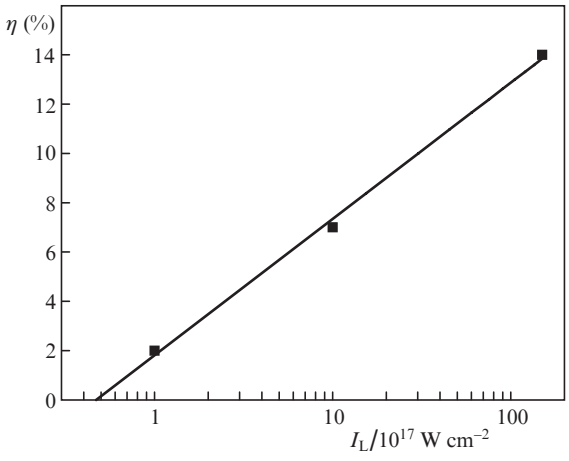

Figure 1. Dependence of the laser energy conversion efficiency into the energy of hot electrons on the intensity: points – calculation by the PIC method [3], solid line – approximation.

tions the following parameters were used: the probabilities $\omega_K = 0.831$ [12] and $p_\alpha = 0.826$ [13], the concentration of atoms $n_a = 5.86 \times 10^{22}$ cm^{-3}, the ionisation potential $E_K = 25.516$ keV and the absorption length $l_a = 74$ μm [14] of K_α radiation with the weighted mean energy of 22.1 keV (defined according to [13, 15]), which correspond to silver under normal conditions.

The K_α yield from the front side of the foil without electron refluxing increases with increasing foil thickness and tends to a constant value (Fig. 2). The maximum K_α yield at an observation angle of 45° is reached at an intensity of 4×10^{18} W cm^{-2}. When reducing observation angle the maximum yield increases slightly (Fig. 3). The K_α yield from the rear side of the foil reaches a maximum at some thickness, which increases with increasing intensity (Fig. 4). At optimal thicknesses and the same observation angle, the K_α yield from the front side of the foil is higher than that from the rear side (Fig. 5).

If electrons are refluxed in the foil, the K_α yield from the front side of the foil increases with increasing intensity and

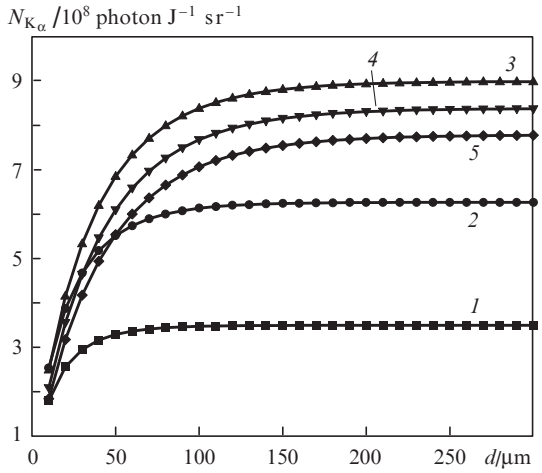

Figure 2. K_α yield from the front side of the foil without electron refluxing as a function of the foil thickness at peak intensities $I_0 = 5 \times 10^{17}$ (*1*), 10^{18} (*2*), 5×10^{18} (*3*), 10^{19} (*4*), and 1.5×10^{19} W cm^{-2} (*5*) and an observation angle $\alpha_0 = 45°$.

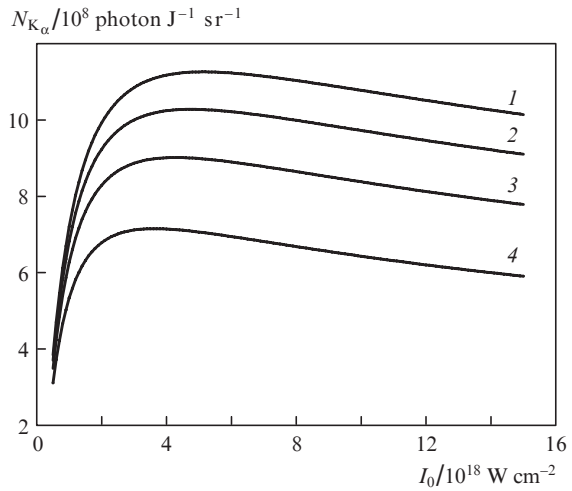

Figure 3. K_α yield from the front side of the 500-μm-thick foil without electron refluxing as a function of the peak intensity at observation angles $\alpha_0 = 0$ (*1*), 30° (*2*), 45° (*3*) and 60° (*4*).

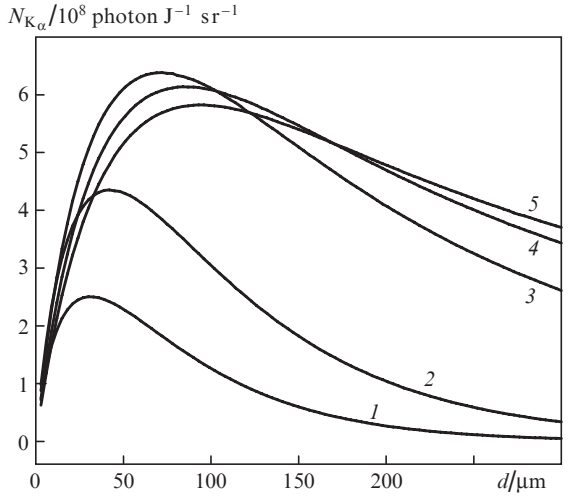

Figure 4. K_α yield from the rear side of the foil without electron refluxing as a function of the foil thickness at peak intensities $I_0 = 5 \times 10^{17}$ (*1*), 10^{18} (*2*), 5×10^{18} (*3*), 10^{19} (*4*), and 1.5×10^{19} W cm^{-2} (*5*) and an observation angle $\beta_0 = 45°$.

decreasing its thickness (Fig. 6). At $I_0 \geqslant 10^{18}$ W cm^{-2} and the same observation angles the K_α yield from the rear side of the foil is less than the yield from the front side with thicknesses greater than the effective absorption length $l_a \cos\alpha_0$ (Fig. 7).

The relative yield of K_α radiation can be measured with greater accuracy than the absolute yield. The ratio of the K_α yields from the front side of a thin and thick foils increases with increasing intensity for the target with the electron refluxing taken into account (Fig. 8) and decreases for the target in which refluxing is insignificant (Fig. 9). This feature can be used to study the effect of electron refluxing, which greatly increases the K_α yield (see Figs 5 and 6).

4. Conclusions

Thus, we have constructed a model of generation of K_α radiation by hot electrons in a foil, which takes into account the spatial dependence of the probabilities of photon emission

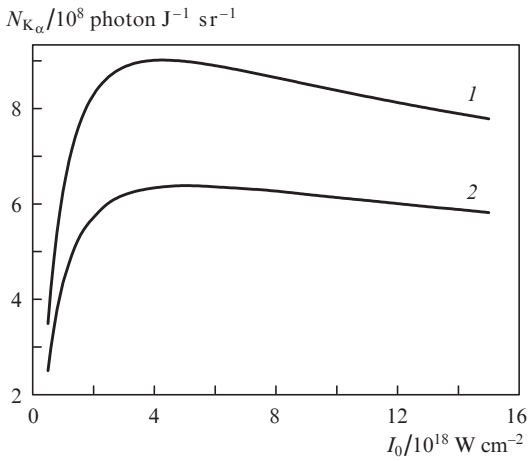

Figure 5. K_α yield from the front (*1*) and rear (*2*) sides of the foil without electron refluxing as a function of the peak intensity at the corresponding optimal thicknesses and observation angles $\alpha_0 = \beta_0 = 45°$.

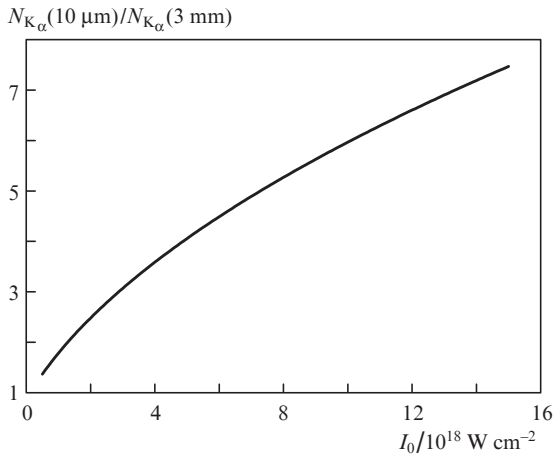

Figure 8. Ratio of the K_α yields from the front side of a thin (10 μm) and thick (3 mm) foils with electron refluxing as a function of the peak intensity at $\alpha_0 = 45°$.

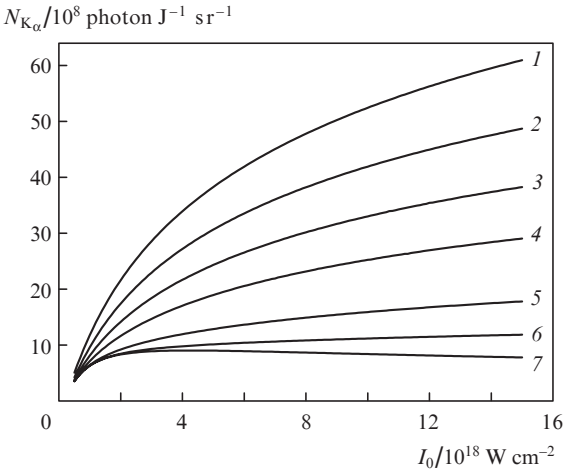

Figure 6. K_α yield from the front side of the foil as a function of the peak intensity with electron refluxing taken into account at the foil thickness $d = 5$ (*1*), 30 (*2*), 60 (*3*), 100 (*4*), 200 (*5*), 360 (*6*), and 3000 μm (*7*) and $\alpha_0 = 45°$.

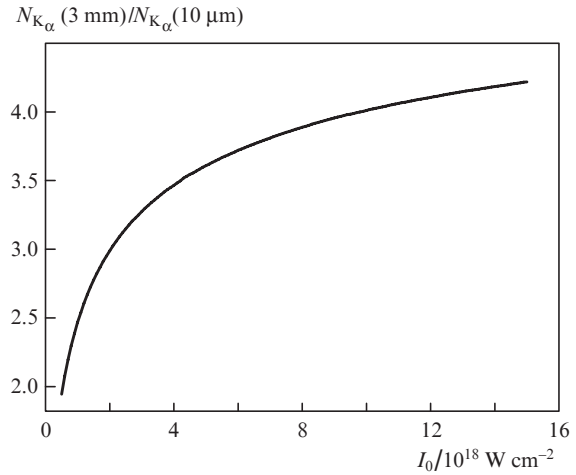

Figure 9. Ratio of the K_α yields from the front side of a thick (3 mm) and thin (10 μm) foils without electron refluxing as a function of the peak intensity at $\alpha_0 = 45°$.

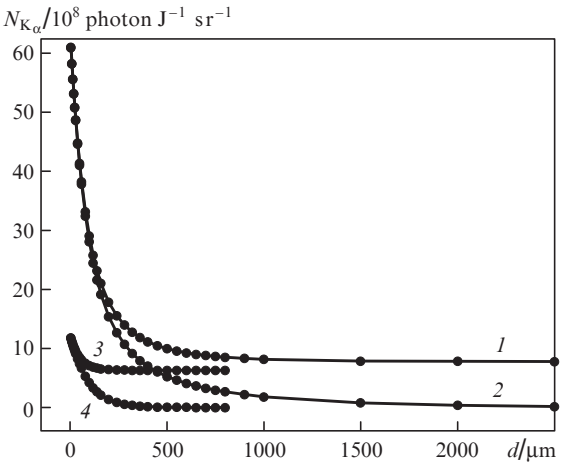

Figure 7. K_α yield from the front (*1*, *3*) and rear (*2*, *4*) sides of the foil as a function of its thickness with electron refluxing taken into account at the peak intensity $I_0 = 1.5 \times 10^{19}$ (*1*, *2*) and 10^{18} (*3*, *4*) W cm^{-2} and $\alpha_0 = \beta_0 = 45°$.

and absorption. This allows the calculation of the anisotropic yield of this emission from the front and back sides of the foil of arbitrary thickness with and without electron refluxing taken into account. We have proposed a method for diagnosing the effect of electron refluxing in the foils, which significantly increases the K_α yield. The calculations and optimisation of the K_α yield allow one to predict and analyse the results of measurements performed on the petawatt laser facilities. The developed model can also be used to refine the results of calculations of the characteristic X-ray yield from the target with a clustered surface [16] and compare them with the results of measurements [17].

Acknowledgements. This work was supported in part by the Programme 'Extreme Light Fields and Their Applications' of the Presidium of RAS and the Russian Foundation for Basic Research (Grant Nos 11-02-91058-CNRS-a and 11-02-12217-ofi-m-2011).

References

1. Wilks S.C., Kruer W.L., Tabak M., Langdon A.B. *Phys. Rev. Lett*., **69**, 1383 (1992).
2. Glenzer S.H., Redmer R. *Rev. Mod. Phys*., **81**, 1625 (2009).
3. Neumayer P., Aurand B., Basko M., et al. *Phys. Plasmas*, **17**, 103103 (2010).
4. Theobald W., Akli K., Clarke R., et al. *Phys. Plasmas*, **13**, 043102 (2006).
5. Myatt J., Theobald W., Delettrez J.A., et al. *Phys. Plasmas*, **14**, 056301 (2007).
6. Kruer W.L., Estabrook K. *Phys. Fluids*, **28**, 430 (1985).
7. Gibbon P. *Short Pulse Laser Interactions with Matter. An Introduction* (London: Imperial College Press, 2005).
8. Berger M.J., Coursey J.S., Zucker M.A., Chang J. *ESTAR, PSTAR, and ASTAR: Computer Programs for Calculating Stopping-Power and Range Tables for Electrons, Protons, and Helium Ions (version 1.2.3)* (Gaithersburg: National Institute of Standards and Technology, 2005).
9. Hombourger C. *J. Phys. B*, **31**, 3693 (1998).
10. Gryzinski M. *Phys. Rev.*, **138**, A322 (1965).
11. Quarles C.A. *Phys. Rev. A*, **13**, 1278 (1976).
12. Krause M.O. *J. Phys. Chem. Ref. Data*, **8**, 307 (1979).
13. Salem S.I., Panossian S.L., Krause R.A. *At. Data Nucl. Data Tables*, **14**, 91 (1974).
14. Henke B.L., Gullikson E.M., Davis J.C. *At. Data Nucl. Data Tables*, **54**, 181 (1993).
15. Bearden J.A. *Rev. Mod. Phys*., **39**, 78 (1967).
16. Kostenko O.F., Andreev N.E. *Contrib. Plasma Phys.*, **51**, 463 (2011).
17. Ovchinnikov A.V., Kostenko O.F., Chefonov O.V., et al. *Laser Part. Beams*, **29**, 249 (2011).